Turbulent Mixing in Stably Stratified Shear Flows

U. SCHUMANN AND T. GERZ

DLR, Institute of Atmospheric Physics, Oberpfaffenhofen, Germany

(Manuscript received 8 October 1993, in final form 2 May 1994)

ABSTRACT

Vertical mixing of momentum and heat is investigated in turbulent stratified shear flows. It is assumed that the flow has uniform shear and stratification with homogeneous turbulence and that an equilibrium is reached between kinetic and potential energy without gravity wave oscillations. A simple model is derived to estimate vertical diffusivities for Richardson numbers in between 0 and about 1. The model is based on the budgets of kinetic and potential energy and assumes a linear relationship between dissipation, shear, and vertical velocity variance for closure. Scalar fluctuations are related to shear or buoyancy frequency depending on the Richardson number. The turbulent Prandtl number and the growth rate of kinetic energy are specified as functions of this number. Model coefficients are determined mainly from laboratory measurements. Data from large-eddy simulations are used to determine the "stationary" Richardson number with balanced shear production, dissipation, and buoyancy terms. The results of the model are compared with data from laboratory experiments in air or saltwater, with measurements in the atmospheric boundary layer and in the stable troposphere, and with results from the numerical simulations. The model interpolates the observations within the scatter of the data. The analysis shows intrinsic relationships between several mixing parameters.

1. Introduction

Stratified shear flows are important in the stratosphere (Sidi and Dalaudier 1990), in the free stable troposphere (Tjernström 1993), in the stable atmospheric boundary layer over cooled surfaces (Nieuwstadt 1984), and in the ocean (Gregg 1987). For many applications, one needs estimates of the rate of turbulent mixing in neutrally and stably stratified shear flows (Fernando 1991). This is a particularly difficult topic because waves may cause turbulence by overturning (Farrell and Ioannou 1993), and turbulence that originated from some strong initial disturbance may decay (Woods 1969) or "collapse" and degenerate to wavy motions under strongly stable stratification (Hopfinger 1987). Often, stable stratified shear flows are strongly oscillating (Einaudi and Finnigan 1993).

In view of the difficulties to determine the level of turbulence and even the mean profiles in stably stratified shear flows, simple relationships are required to estimate the magnitude of the mixing properties. Such relationships have been deduced, mainly for strongly stratified atmospheric and oceanic flows, on the basis of the energy budgets using simple closure assumptions for stationary flows, for example, by Lilly et al. (1974), Osborn (1980), and Hunt et al. (1985). The present paper extends these models and a preliminary version given in Schumann (1994). It takes into account the deviation from stationarity and applies to both stratified and unstratified shear flows.

Turbulence in stratified shear flows depends strongly on the Richardson number. For convenience, we specify this number and the subsequent theory for thermal stratification but will also discuss density variations due to variable salt concentration in water. Hence, we consider the turbulence properties of a flow with given vertical velocity shear S and positive vertical potential temperature gradient s,

$$S = \frac{dU}{dz}, \quad s = \frac{d\Theta}{dz}, \tag{1}$$

which define the Brunt–Väisälä frequency N and the gradient Richardson number Ri,

$$N = (\beta g s)^{1/2}, \quad \mathrm{Ri} = \frac{N^2}{S^2}. \tag{2}$$

Here, β is the thermal volumetric expansion coefficient, and g is the acceleration of gravity. For $\mathrm{Ri} < 0.25$ somewhere in the flow, small perturbances in inviscid fluid may grow exponentially (Miles 1961). In general, one expects that existing turbulence decays with time when $\mathrm{Ri} > 0.25$ (Woods 1969). In viscous flows this limit may be smaller (Nieuwstadt 1984). But even for $\mathrm{Ri} = O(1)$, transient growth of perturbations can be substantial and may cause overturning for $\mathrm{Ri} < 0.4$ (Farrell and Ioannou 1993). Turbulent motions get enhanced by shear at small Richardson numbers and the kinetic energy in homogeneous turbulence grows about exponentially with time for zero Richardson

Corresponding author address: U. Schumann, DLR, Institute of Atmospheric Physics, 82230 Oberpfaffenhofen, Germany.

number (Tavoularis and Karnik 1989). Hence, turbulent mixing may occur under nonstationary conditions at all Richardson numbers.

When comparing mixing properties in the atmosphere and in the ocean, one has to note the rather large molecular Schmidt number of salt diffusing in water (about 500) while the corresponding Prandtl number of thermal diffusion in air is about 0.7. At high Reynolds numbers, one generally expects that the large-scale turbulent motions become independent of the Prandtl number, at least for neutral stratification. However, for strong stratification, Pearson et al. (1983) show that the vertical diffusivity is limited by small-scale mixing once the available kinetic energy is consumed to provide the potential energy required for vertical displacements. Such small-scale processes will depend on molecular diffusion.

The present theory uses several assumptions in order to allow for a simple analytical model. It assumes that the density variations affect the buoyancy only, that is, we employ the Boussinesq approximation. The analysis is restricted to flows at high Reynolds numbers with active turbulence and with small molecular diffusion at the energy containing scales. The turbulence is further assumed to be strongly sheared ($\mathrm{Ri} < 1$) so that the timescale S^{-1} of shear is smaller than the timescale N^{-1} of stratification, and both should be smaller than the turbulence timescales. The theory assumes a homogeneously turbulent flow exposed to uniform (linear) vertical shear and stratification. Because of homogeneity, all divergences of fluxes vanish so that also the mean profiles do not change due to turbulent mixing. As a result, the mean flow is characterized by an unique value of Ri. The assumption of *nearly* homogeneous turbulence is appropriate when the length scales of turbulence are small compared to outer scales of any variations in the mean profile such that the divergence of fluxes is small compared to the local rate of energy dissipation. By means of scale analysis, Mellor and Yamada (1974) have shown that this assumption of nearly homogeneous turbulence is often satisfied even in inhomogeneous boundary layers. Finally, we assume that the exchange of energy between its kinetic and potential form has approached a local equilibrium so that averaged quantities decay in a nonoscillating manner. Hence, the model excludes situations with large amplitude wavy oscillations between kinetic and potential forms of energy.

Homogeneous turbulence is by necessity time dependent and becomes stationary only under special conditions near a "stationary" Richardson number. Certainly, the transient states at other Richardson numbers cannot last forever. For stable stratification the energy will decay and disappear until any event, which the present model will not explain, creates a new turbulent region. The model loses validity when the turbulence gets so weak that viscosity becomes important. For growing turbulence in a large but finite domain, the assumption of homogeneity eventually breaks down when growing spatial gradients cause substantial energy diffusion out of the finite turbulent region.

Homogeneous turbulent shear flows have been measured by Rohr et al. (1988) in salt-stratified water. Their data are taken from appendix 2 of Rohr (1985) at shear times $tdU/dz > 6$ when the flow has approached constant correlation coefficients. Reliable data for homogeneous air flows are available only for neutral stratification (Tavoularis and Karnik 1989). In order to extend the database, we use results from numerical simulations of three-dimensional turbulence in homogeneous stratified shear flows at a Prandtl number of one.

Homogeneous turbulence in stratified shear flows has been investigated by direct numerical simulation (DNS) in Gerz et al. (1989), Gerz and Schumann (1991), and Holt et al. (1992). They investigated the flow dynamics as a function of Richardson numbers in between 0 and 1.32. DNS on grids with 128^3 grid points, as we could realize for this study, is typically restricted to a Prandtl number of order unity and to a turbulent Reynolds number, based on root-mean-square velocity fluctuations and Taylor's microscale, of less than about 50. For atmospheric flows, much larger Reynolds numbers are of interest. For this reason, the DNS method has been extended by Kaltenbach (1992) into a large-eddy simulation (LES) using a simple subgrid-scale model (Lilly 1967). This extends formally the Reynolds number to infinity. However, the range of resolved scales is still limited by numerical resolution. The method and the parameters used for LES are summarized in the appendix. Details and further results are reported in Kaltenbach et al. (1994). These are the first LES of stably stratified sheared homogeneous turbulence. LES of turbulence in the stable atmospheric boundary layer have been performed by Mason and Derbyshire (1990), and these results have been used by Derbyshire and Hunt (1993) to investigate mixing models.

The paper is organized as follows. In section 2, a simple theory is deduced based on the budget of kinetic energy. Here, temperature fluctuations are assumed to be correlated with shear for small Richardson numbers and with stratification for large Richardson numbers. The results of this model are compared to several experiments and to the results of the LES. Section 3 extends the model using the budget of potential energy to determine the dependence of temperature fluctuations on Richardson number. Section 4 discusses various assumptions and consequences of the model and shows that the results are not far from measurements in the stationary but inhomogeneous boundary layer and in some stratified flows with weak shear. Finally, section 5 summarizes the conclusions.

2. A simple model based on the budget of kinetic energy

a. *Definitions and consequences of the budget of kinetic energy*

In homogeneous turbulence the ensemble averaged kinetic energy $E_k = 0.5(\overline{u^2} + \overline{v^2} + \overline{w^2})$ of the turbulent velocity fluctuations is a pure function of time t, and satisfies the budget

$$\frac{dE_k}{dt} = P - B - \epsilon. \tag{3}$$

It states that the local rate of change in kinetic energy equals the sum of shear production P, buoyancy destruction B, and viscous dissipation ϵ. If vertical shear and stratification dominate, the production terms are functions of the vertical turbulent fluxes of momentum and heat and of the related turbulent diffusivities,

$$P = -\overline{uw}S = K_m S^2, \quad B = -\frac{\overline{w\theta}N^2}{S} = K_h N^2. \tag{4}$$

Their ratio defines the flux Richardson number Ri_f and the turbulent Prandtl number Pr_t,

$$\mathrm{Ri}_f = \frac{B}{P} = \frac{\mathrm{Ri}}{\mathrm{Pr}_t}, \quad \mathrm{Pr}_t = \frac{K_m}{K_h}. \tag{5}$$

Now, we introduce the parameter G,

$$G = \frac{P}{\epsilon + B}, \tag{6}$$

which controls the growth rate of kinetic energy,

$$\frac{dE}{dt} = (G - 1)(\epsilon + B). \tag{7}$$

The growth rate G is positive for downgradient mixing, $G = 1$ for stationary flows, $G = 0$ for decaying flows without shear production, and $G = P/\epsilon$ in neutral shear flows. As a consequence of the budget of kinetic energy and the above definitions of Ri_f and G, the rates of shear forcing and buoyancy destruction are related to the rate of dissipation by

$$B = \frac{\mathrm{Ri}_f G}{1 - \mathrm{Ri}_f G}\epsilon, \quad P = \frac{G}{1 - \mathrm{Ri}_f G}\epsilon. \tag{8}$$

Together with Eq. (4), these relationships determine the turbulent diffusivities,

$$K_m = c_m \frac{\epsilon}{S^2}, \quad c_m = \frac{G}{1 - \mathrm{Ri}_f G}, \tag{9}$$

$$K_h = c_h \frac{\epsilon}{N^2}, \quad c_h = \frac{\mathrm{Ri}_f G}{1 - \mathrm{Ri}_f G}. \tag{10}$$

The coefficient c_h is often quoted as the "mixing efficiency" (Weinstock 1992). One also obtains estimates for the "stress coefficient" and for the correlation coefficient of the heat flux,

$$\alpha_{uw} \equiv -\frac{\overline{uw}}{w'^2} = c_m \frac{\epsilon}{w'^2 S}, \tag{11}$$

$$\alpha_{w\theta} \equiv -\frac{\overline{w\theta}}{w'\theta'} = c_h \frac{\epsilon S}{N^2 w'\theta'} = \frac{c_m}{\mathrm{Pr}_t}\frac{\epsilon S}{S^2 w'\theta'}, \tag{12}$$

where $w' = (\overline{w^2})^{1/2}$ and $\theta' = (\overline{\theta^2})^{1/2}$ are the root-mean-square values of the turbulent fluctuations of vertical velocity and temperature. Except for $\alpha_{w\theta}$, which depends also on θ', all other terms are determined once ϵ, w', S, N, G, and Pr_t are given.

b. *Approximations for dissipation and scalar fluctuations*

According to Hunt et al. (1988), for stratified shear flows, the dissipation due to small-scale mixing in turbulent flows (remote from boundaries) is controlled by the shear rate S and by w', the characteristic velocity in the direction of the mean gradients. Dimensional analysis and Prandtl's classical eddy mixing concept suggest

$$\epsilon = A_S w'^2 S, \tag{13}$$

with A_S as a yet undetermined model coefficient. This model looks similar to classical dissipation closure models when written as $\epsilon = A_S w'^3/l_w$, but fixes the mixing length as $l_w = w'/S$. This appears to be natural for strongly sheared flows. Hunt et al. (1988) suggested that this model gives a good approximation for $0 \leqslant \mathrm{Ri} < 0.5$. We will show that this is supported by various measurements and by the LES results and that the upper limit may even reach up to $\mathrm{Ri} = O(1)$.

Most of the temperature fluctuations originate from turbulent motions at the large scales and are more sensitive to buoyancy, therefore. Hence, the impact of buoyancy gets important at values of Ri considerably less than 1. Dimensional analysis and order of magnitude estimates give

$$\theta' = \begin{cases} \dfrac{\zeta_S w' S}{S}, & \mathrm{Ri} \leqslant 0.25 \\ \dfrac{\zeta_N w' S}{N}, & \mathrm{Ri} > 0.25 \end{cases}. \tag{14}$$

Here, ζ_S, and ζ_N are yet open coefficients. The first relationship can be understood from the mixing concept, which suggests $\theta' \cong l_\theta S$ and $w' = l_w S$, with $\zeta_s = l_\theta/l_w$ as the ratio of relevant mixing lengths. A reduction of ζ_S appears reasonable at large Richardson numbers where the vertical scale l_θ of temperature fluctuations is affected by buoyancy more strongly than the scale of vertical motions l_w. In fact, the scaling with N instead of S at strong stratification accounts for the balance between kinetic and potential energy, as will be discussed further in section 3. Previous authors have often

used the scaling with N even at small values of Ri, where we expect that shear becomes the dominant parameter. The limit Ri = 0.25 is certainly only approximately valid and is taken in correspondance with the linear stability criterion of inviscid flows.

The two versions for the temperature fluctuations given in Eq. (14) are consistent with each other if

$$\zeta_S = \text{const}, \quad \zeta_N = \zeta_S \, \mathrm{Ri}^{1/2}, \tag{15}$$

for $\mathrm{Ri} \leq 0.25$, and

$$\zeta_S = \zeta_N \, \mathrm{Ri}^{-1/2}, \quad \zeta_N = \text{const}, \tag{16}$$

for $\mathrm{Ri} > 0.25$, with $\zeta_N = 0.5\zeta_S$ at the limit between the two ranges. Hence, only one of these coefficients is an independent model parameter.

These relations are introduced into Eqs. (9)–(12), to obtain

$$\alpha_{uw} = c_m A_S = \frac{A_S G}{1 - \mathrm{Ri}_f G}, \tag{17}$$

$$\alpha_{w\theta} = \frac{\alpha_{uw}}{\zeta_S \, \mathrm{Pr}_t}, \tag{18}$$

$$K_h = \frac{c_S w'^2}{S} = \frac{c_N w'^2}{N}, \quad K_m = K_h \, \mathrm{Pr}_t, \tag{19}$$

with

$$c_S = \frac{\alpha_{uw}}{\mathrm{Pr}_t}, \quad c_N = \frac{\alpha_{uw} \, \mathrm{Ri}^{1/2}}{\mathrm{Pr}_t}. \tag{20}$$

We remark that ζ_S affects the correlation coefficient $\alpha_{w\theta}$ but not the diffusivities.

c. Closure assumptions

In order to close the set of equations, one needs to specify A_S and ζ_S or ζ_N as well as the growth-rate parameter $G(\mathrm{Ri})$, and the turbulent Prandtl number $\mathrm{Pr}_t(\mathrm{Ri})$, which we assume to be pure functions of Ri. This assumption is similar to assuming that the flux Richardson number is a unique function of the gradient Richardson number, as commonly assumed for boundary layer flows (Nieuwstadt 1984). One expects that G and Pr_t are not unique functions of Ri but depend also on the ratio of outer to inner (turbulent) timescales, such as the turbulent Froude number (Ivey and Imberger 1991) or the turbulent shear number (Tavoularis and Karnik 1989). But we will see (in sections 4b and 4c) that these numbers are related to Ri or become constant when the turbulent timescale is large.

The function $G(\mathrm{Ri})$ is set up such that it equals the value $G_0 = P/\epsilon > 1$ for neutral shear flows at Ri = 0, becomes unity at the stationary Richardson number Ri_s, for which the forcing by shear just balances dissipation and buoyancy destruction, and decreases at large Richardson numbers, where shear production of energy cannot balance dissipation and buoyant destruction. This can be expressed by a monotonic function that approaches zero at large Richardson numbers. We select the exponential function for simplicity,

$$G = G_0^{(1-\mathrm{Ri}/\mathrm{Ri}_s)}. \tag{21}$$

This function does not necessarily imply an exponential decay of energy with time. In fact, the present model predicts exponential increase or decay only when $w'^2/E_k = \text{const}$. The value of Ri_s is less than the inviscid stability limit 0.25 because of finite dissipation in real flows (see Nieuwstadt 1984).

Several conflicting theories and measurements exist for the turbulent Prandtl number. As will be discussed in section 4d, the value Pr_{t0} for neutral flows varies typically in between 0.7 and 1.2. Also, the data suggest that Pr_t is fairly insensitive to stratification as long as Ri is small. Because of $\mathrm{Pr}_t = \mathrm{Ri}/\mathrm{Ri}_f$, and finite value of Ri_f, we expect that Pr_t increases with Ri. Some measurements and numerical simulations (see Gerz et al. 1989) show that Pr_t grows strongly with Ri and may even become infinite when the heat flux and Ri_f approach zero at the transition to wavy flows. However, for equilibrium flows, it appears reasonable to assume that Pr_t stays finite at all Richardson numbers, and varies as

$$\mathrm{Pr}_t = \mathrm{Pr}_{t0} \exp\left(-\frac{\mathrm{Ri}}{\mathrm{Pr}_{t0} \, \mathrm{Ri}_{f\infty}}\right) + \frac{\mathrm{Ri}}{\mathrm{Ri}_{f\infty}}. \tag{22}$$

This equation is constructed such that Pr_t increases with zero gradient at Ri = 0. At large values of Ri, $\mathrm{Pr}_t \to \mathrm{Ri}/\mathrm{Ri}_{f\infty}$. Here, we assume that the value of Ri_f approaches a constant limit $\mathrm{Ri}_{f\infty}$. The data do not allow to determine this parameter very precisely, and the value $\mathrm{Ri}_{f\infty} = 0.25$, which we select, is probably an upper limit, but not far from 0.2 as found by Nieuwstadt (1984).

d. Determination of the model coefficients

The coefficients are fixed using mainly the previously discussed laboratory data (see Schumann 1994). Table 1 contains the LES results, which are used to determine the stationary Richardson number. The mean values of the measurements have been tabulated in Schumann (1994). We find that the coefficients differ depending on the molecular Prandtl number (or Schmidt number), as was to be expected. In saltwater, the damping of concentration fluctuations is much smaller than that of temperature fluctuations in air. Therefore, we have to give two sets of coefficients. For saltwater we use the measurements of Rohr (1985). For Ri = 0, the data give $G_0 = P/\epsilon = 1.8 \pm 0.36$ and $\alpha_{uw} = 0.87 \pm 0.08$. Hence, Eq. (17) implies $A_S = \alpha_{uw}/G_0 = 0.48$. For Ri = 0, also the value $\zeta_S = 2.88 \pm 0.15$ is measured, giving $\zeta_N = \zeta_S/2 = 1.44$. The scalar flux correlation coefficient was found to be $\alpha_{w\theta} = 0.42 \pm 0.03$. From Eq. (18), we

TABLE 1. Large-eddy simulation results: Mean values and standard deviations.

Ri	0	0.13	0.25	0.5	1.0
$P(B+\epsilon)^{-1}$	1.54 ± 0.048	0.999 ± 0.031	0.632 ± 0.021	0.190 ± 0.036	−0.031 ± 0.015
$-\overline{uw}w'^{-2}$	0.829 ± 0.046	0.703 ± 0.020	0.532 ± 0.011	0.157 ± 0.037	−0.036 ± 0.007
$-\overline{w\theta}(w'\theta')^{-1}$	0.467 ± 0.006	0.323 ± 0.010	0.187 ± 0.004	0.031 ± 0.008	−0.013 ± 0.007
$\theta' S(w's)^{-1}$	2.38 ± 0.03	2.80 ± 0.03	2.75 ± 0.03	2.26 ± 0.02	1.54 ± 0.01
$\epsilon(w'^2 S)^{-1}$	0.540 ± 0.016	0.587 ± 0.027	0.638 ± 0.015	0.635 ± 0.025	0.508 ± 0.045
Pr_t	0.741 ± 0.033	0.781 ± 0.041	1.03 ± 0.014	2.28 ± 0.25	—
$w'^2 q^{-2}$	0.183 ± 0.009	0.149 ± 0.003	0.140 ± 0.004	0.137 ± 0.004	0.153 ± 0.004

conclude $\mathrm{Pr}_{t0} = \alpha_{uw}(\alpha_{w\theta}\zeta_S)^{-1} = 0.72$. For Ri > 0, the data suggest $G(0.36) = 0.5 \pm 0.3$, which defines $\mathrm{Ri}_s \cong 0.16 \pm 0.06$.

Similarly, for air we take the wind tunnel data of Tavoularis and Corrsin (1981, 1985) and Tavoularis and Karnik (1989), for Ri = 0, to obtain $G_0 = 1.47 \pm 0.13$, $\alpha_{uw} = 0.73 \pm 0.05$, $\alpha_{w\theta} = 0.45 \pm 0.03$, and $\zeta_S = 1.65 \pm 0.1$. Hence, $A_S = 0.50$, $\zeta_N = 0.825$, and $\mathrm{Pr}_{t0} = 0.98$. No measurements exist for homogeneous turbulence in airflows at Ri > 0, but from the LES, which were performed with a comparable subgrid-scale Prandtl number of 1, we determine $\mathrm{Ri}_s \cong 0.13$. The resultant model coefficients are summarized in Table 2.

e. *Comparison to measurements and simulation results*

Figure 1 shows that a constant value of $A_S = \epsilon(w'^2 S)^{-1}$ falls within the error band of the measurements of Rohr (1985) for salt diffusing in water and of Tavoularis and Karnik (1989) for thermal diffusion in air. The differences between A_S for air and saltwater are insignificant. The value of A_S is remarkably close to the value 0.45 deduced in Hunt et al. (1988) from the logarithmic law of the wall in the neutral boundary layer. The LES results do roughly confirm the derived value of A_S.

The growth rate G is plotted versus Ri in Fig. 2. The scatter of the individual measurements is quite large. Nevertheless, the data support the assumed exponential trend, with $G \cong 0$ at Ri = 1, in particular when one includes the LES results (see Table 1). In principle, there is no reason why $G(0) = G_0$ should be different in air and saltwater flows. However, the differences are within the scatter of the data. The stationary Richardson number Ri_s, for which $G = 1$, is obviously difficult to determine very precisely. From DNS, Holt et al. (1992) found Ri_s growing from 0.05 to 0.21 with increasing Reynolds number. The LES result $\mathrm{Ri}_s = 0.13$ for air is, perhaps incidentally, close to the DNS results obtained by Gerz and Schumann (1991). This value is little smaller than the generally accepted values of 0.2 or 0.22 for stably stratified air flows (Nieuwstadt 1984). It appears possible that this difference is due to deviations from homogeneity, as will be discussed in section 4f. Compared to saltwater, a smaller value of Ri_s has to be expected in air because of the enhanced dissipation of total energy (kinetic and potential) by the stronger thermal diffusion at the smaller Prandtl number.

The dependence of the turbulent Prandtl number Pr_t on Ri is depicted in Fig. 3. The data from the measurements and from the LES are in rough agreement with the interpolation curves for water and air. (The dotted curve will be discussed in section 4e.) Kim and Mahrt (1992) fit their measurements in the stable lower troposphere by $\mathrm{Pr}_t = 1 + \mathrm{Ri}/0.263$. This function is close to the present assumption showing also a linear trend at large values of Ri. It implies a value 0.263 for

TABLE 2. Model parameters for air and saltwater.

Coefficient	Air	Salt
A_S	0.50	0.48
ζ_S	1.65	2.88
G_0	1.47	1.80
Ri_S	0.13	0.16
Pr_{t0}	0.98	0.72

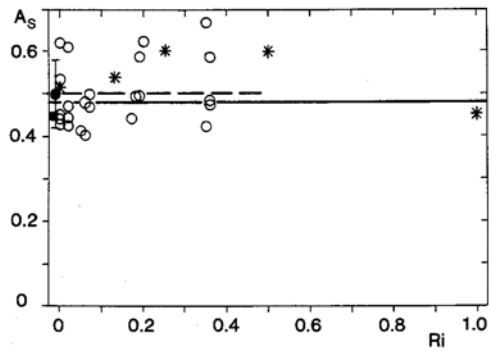

FIG. 1. Dissipation scaled by shear and vertical velocity variance, $A_S = \epsilon(w'^2 S)^{-1}$ versus gradient Richardson number Ri, based on the data of Rohr (1985) in saltwater (circles), the measurements in neutrally stratified wind tunnel shear flows of Tavoularis and Karnik (1989) (full circle with error bar), and the LES results (stars). The full line corresponds to the present model, Eq. (13), for air, the dashed line represents the best fit for the saltwater data. The square dot at Ri = 0 indicates the boundary layer estimate by Hunt et al. (1988).

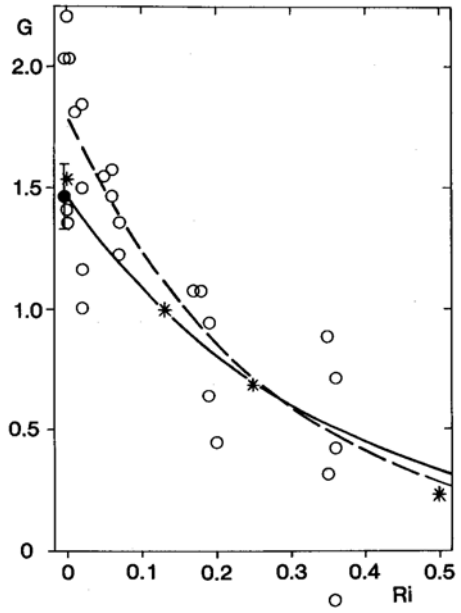

FIG. 2. Growth factor $G = P(B + \epsilon)^{-1}$ versus Ri. Symbols as in Fig. 1. The full curve depicts Eq. (21) for air, the dashed curve for saltwater.

$Ri_{f\infty}$, in fair agreement with the value 0.25 that we selected. Tjernström (1993) also tests linear functions but finds that $Pr_t = (1 + 4.47\ Ri)^{1/2}$ fits his data best. Such a function would imply that Ri_f increases with $Ri^{1/2}$ in strongly stratified flows, but we do not see a reason to support such an increase. Schumann (1991) shows that a linear increase of Pr_t for large Ri is necessary to avoid the kinetic energy becoming negative from excessive buoyancy destruction. However, we should note that the turbulent Prandtl number measures the ratio of two diffusivities that are both very small (or even ill conditioned) at high Richardson numbers. Rohr's data show very large variations in the turbulent Prandtl number already for Ri = 0.36, with Pr_t in between −0.6 and 3.4.

Figure 4 shows the resultant trend of the stress coefficient α_{uw} versus Ri. Obviously, the model is a fair approximation in the whole range of Richardson numbers up to 0.5. As an independent source of data, the results from Nieuwstadt (1984) have been included in this plot. Here and in the following figures, the error bars to his data measure the standard deviation between various mean values and not the larger scatter within a single time series. His data agree well with the model, although they are taken from a stationary nonhomogeneous stably stratified atmospheric boundary layer. This fact will be discussed in section 4f. The results show clearly the decreasing trend of the mixing fluxes with Ri.

The ratio $\zeta_S = \theta' S / w' s$ is plotted in Fig. 5. Here, the differences between air and saltwater are very large, but this seems to be justified by the large impact of molecular damping on the magnitude of the scalar fluctuations. The LES data are closer to the measurements in saltwater than to those measured in air, which cannot be explained easily and which indicates that the present concept might not yet cover all influences (as discussed in section 3). For Ri > 0.25, the figure actually depicts $\zeta_S = \zeta_N\, Ri^{-1/2}$. The value $\zeta_N = 0.825$ for air is very close to the values $\zeta_N = 0.8 \pm 0.25$ and $\zeta_N \cong 0.96$ found for the stable atmospheric boundary layer in Nieuwstadt (1984) and Hunt et al. (1985). Recently, Derbyshire and Hunt (1993) deduced from a similar analysis, $\zeta_N = 0.9 \pm 0.1$, for Ri ⩾ 0.2, and $\zeta_N = (2 \pm 0.2)Ri^{1/2}$, for Ri < 0.2. These estimates were shown to compare well with results from LES of the stably stratified boundary layer (Mason and Derbyshire 1990). Hence, these findings are roughly consistent with the present model.

In Fig. 6, the approximations are compared with the data for air and saltwater in terms of the correlation coefficient for vertical scalar fluxes. The curves are the consequences of the previous assumptions, and the data for Ri > 0 have not been used to calibrate the model parameters. Therefore, the comparison provides a check for the internal consistency of the present model and supports the selected value $Ri_{f\infty} = 0.25$. We see that the agreement is generally within the range of the data. The agreement is again very good with respect to the data measured by Nieuwstadt (1984). The heat

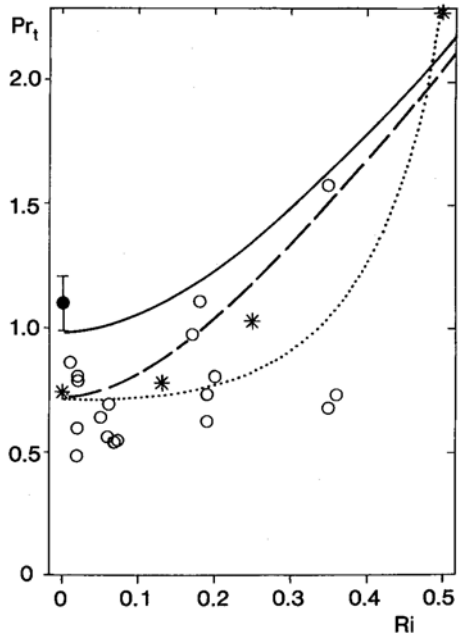

FIG. 3. Turbulent Prandtl number $Pr_t = K_m/K_h$ versus Ri. Symbols as in Fig. 1. The full curve depicts Eq. (22) for air, dashed curve for saltwater. The dotted curve represents Eq. (36) for $Pr_{t0} = 0.72$ and $Ri_f = 0.66$.

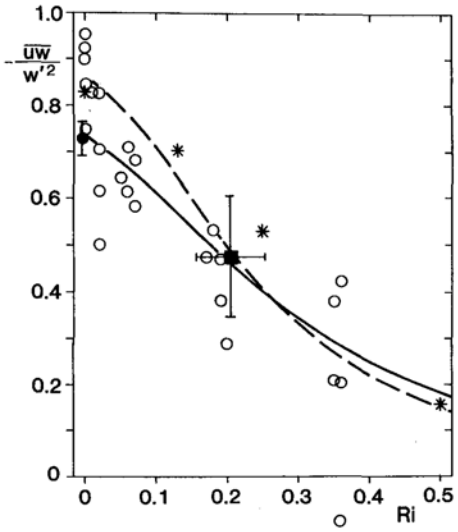

FIG. 4. Stress coefficient $\alpha_{uw} = -\overline{uw}/w'^2$ versus Ri. Symbols as in Fig. 1. In addition the measurements of Nieuwstadt (1984) obtained in the stable atmospheric boundary layer are indicated by the full square with error bars. Full curve, Eq. (17) for air; dashed curve, same for saltwater.

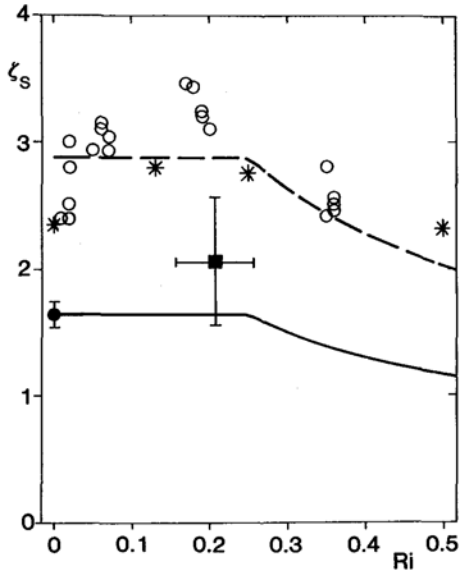

FIG. 5. Temperature fluctuations normalized by shear, temperature gradient, and vertical velocity fluctuations, $\zeta_S = \theta' S/w's$ versus Ri. Symbols as in Fig. 4. Full curve represents Eq. (15) for Ri $\leq$ 0.25, and Eq. (16) for Ri > 0.25 for air; the dashed curve applies for saltwater.

flux decays with increasing Ri more quickly than the momentum flux, which is consistent with an increasing turbulent Prandtl number because of more efficient momentum than heat transport in wavy flows. This can be understood physically (Tritton 1977): "A fluid particle that is displaced but then falls back to its original position without any mixing with its new environment does not transfer any heat, but it can transfer momentum through the action of pressure forces."

3. Estimate of potential energy from its budget

In the above model, we have introduced the values of ζ_N and ζ_S in a purely empirical manner. A slightly more formal support and a refinement to this approximation can be obtained by using the budget of potential energy $E_p = \overline{\theta'^2} N^2/2s^2$,

$$\frac{dE_p}{dt} = B - \epsilon_p. \tag{23}$$

The budget includes the source of potential energy from upward buoyancy flux and the dissipation ϵ_p of potential energy due to small-scale scalar fluxes. This budget can be used to deduce independent estimates of the ratios

$$\eta = \zeta_N^2 = E_p\left(\frac{w'^2}{2}\right)^{-1}, \quad \text{and} \quad \zeta_S^2 = \frac{\eta}{\mathrm{Ri}}. \tag{24}$$

For that purpose, it is assumed that both forms of energy, E_p and E_k, decay at the same rate. Actually, we would need to consider only the ratio of E_p to the kinetic energy of the vertical velocity variance. However, since we have no closed budget for that variance (which would require to specify the pressure-strain term), we start in using the budget of the total kinetic energy instead. Thus, we assume that the ratio

$$\frac{dE_p/dt}{dE_k/dt} = \frac{E_p}{E_k}, \tag{25}$$

stays constant with time. Moreover, it is assumed that the dissipation timescales $\tau = 2E_k/\epsilon$ and $\tau_p = 2E_p/\epsilon_p$ equal a time-independent ratio $Z = \tau/\tau_p$ (which may depend on Ri), that is,

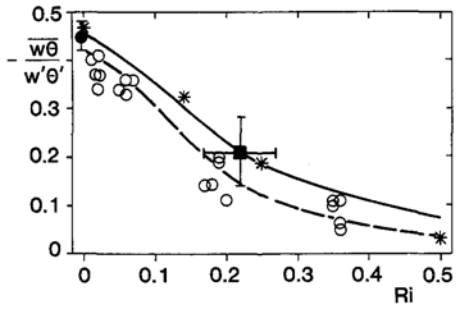

FIG. 6. Vertical scalar flux correlation coefficient $\alpha_{w\theta} = -\overline{w\theta}/w'\theta'$ versus Ri. Symbols as in Fig. 4. Full curve, Eq. (18) for air; dashed curve, same for saltwater.

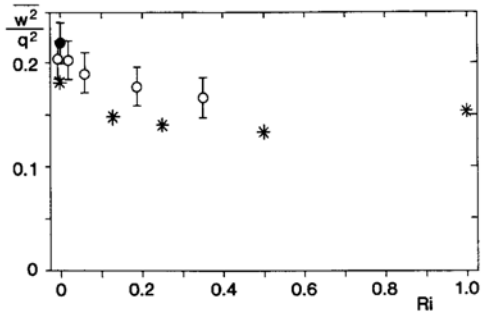

FIG. 7. Vertical velocity variance w'^2 relative to twice the kinetic energy of turbulent velocities $q^2 = u'^2 + v'^2 + w'^2$ versus Ri. Data from Rohr (1985) in saltwater (circles with error bars), from Tavoularis and Corrsin (1985) for air (full circle with error bar), and the LES results (stars).

$$\frac{\epsilon_p}{\epsilon} = Z\frac{E_p}{E_k}. \tag{26}$$

If these assumptions are put into the budget of potential energy, and if B is expressed as in Eq. (8), then one finds that the ratio of potential to kinetic energies is given by

$$\frac{E_p}{E_k} = \frac{\mathrm{Ri}_f}{1 - \mathrm{Ri}_f Z + (Z-1)G^{-1}}. \tag{27}$$

It shows that for $\mathrm{Ri} \gg 1$, where $G \to 0$, a constant ratio of energies can exist only if the ratio of timescales Z approaches unity in the way that

$$Z = 1 + \xi G, \tag{28}$$

with a parameter ξ of finite value.

In order to evaluate η under these conditions, we need to know the ratio of vertical to total kinetic energy, w'^2/q^2, with $E_k = q^2/2$. If this ratio is given and if ξ is a parameter that is independent of Ri, then ξ can be determined from

$$\xi = \frac{q^2}{w'^2}\frac{1}{\mathrm{Pr}_{t0}\zeta_S^2} - 1, \tag{29}$$

for Ri = 0, which follows from Eqs. (27) and (28). Hence, ξ and then Z and ζ_N are determined once the parameters Pr_{t0} and ζ_S are given at Ri = 0 and if the function q^2/w'^2 is given for all Ri.

Figure 7 shows data that are available on the ratio of energies w'^2/q^2 for homogeneous turbulence. Basically, one has to expect that this ratio depends not only on Ri but also on the relative importance of wavy and vortical flow components. Nevertheless, the few available data allow only to determine a dependence on Ri, such as

$$\frac{w'^2}{q^2} = 0.15 + 0.07\exp\left(-\frac{\mathrm{Ri}}{0.25}\right) + 0.02\,\mathrm{Ri}, \quad \text{for air,} \tag{30}$$

$$\frac{w'^2}{q^2} = 0.15 + 0.05\exp\left(-\frac{\mathrm{Ri}}{0.25}\right) + 0.02\,\mathrm{Ri}, \quad \text{for salt in water.} \tag{31}$$

The conclusions do not change much if a constant value $w'^2/q^2 = 0.22$ is used.

As a consequence of the previously determined parameters, we get $\xi = 0.70$ for air and $\xi = -0.16$ for salt. The sign of ξ determines whether Z is larger or smaller than unity. For Ri = 0, the given values imply $Z = 1.98$ for air and $Z = 0.75$ for salt. Hence, the theory predicts a drastically smaller ratio $Z = \tau/\tau_p$ of dissipation timescales for air than for saltwater. This appears to be a reasonable consequence of the differences in molecular Prandtl and Schmidt numbers and agrees qualitatively with simulation results of Gerz et al. (1989).

Figure 8 shows the resultant ratio

$$\eta = \frac{q^2}{w'^2}\frac{\mathrm{Ri}_f}{1 - \mathrm{Ri}_f(1 + \xi G) + \xi} \tag{32}$$

versus Richardson number by the thick curves, where w'^2/q^2 is computed from Eqs. (30) and (31). The thin

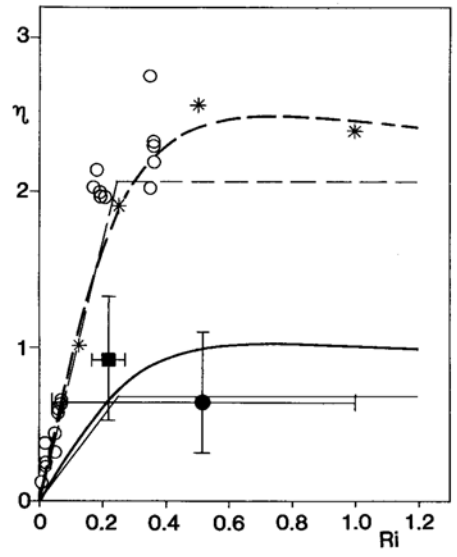

FIG. 8. Potential energy over kinetic energy of vertical motions, $\eta = N^2\theta'^2/s^2w'^2$, versus Ri. Data from Rohr (1985) in saltwater (circles), from the LES results (stars), from Nieuwstadt (1984) (full square with error bars), and from Hunt et al. (1985) (full circle with bars indicating the maximum variations of the measured data). The thick curve depicts the model, Eq. (32) for air; the dashed curve is the result for saltwater. The thin straight lines correspond to $\eta = \mathrm{Ri}\zeta_S^2$ for $\mathrm{Ri} \leq 0.25$, and $\eta = \zeta_N^2$ for $\mathrm{Ri} > 0.25$, according to Eqs. (15) and (16), and Table 2.

lines depict the simple approximations in terms of $\eta = \zeta_S^2 \mathrm{Ri}$, for $\mathrm{Ri} \leq 0.25$, and $\eta = \zeta_N^2 = \zeta_S^2/4 = \text{const}$ for stronger stratification, using the respective value of ζ_S listed in Table 2. Moreover, the figure includes the data points from Rohr (1985) and the results of Nieuwstadt (1984). The widely scattering data from Hunt et al. (1985) are within the range included by the bars. Roughly speaking, the interpolations given by the curves fit the data to within the uncertainty of the measurements.

The thin lines show qualitatively the same trends as the full curves. Incidentally, the agreement would be even better if the full curves would be computed from Eq. (32) with $w'^2/q^2 = 0.22$. Anyway, the general agreement confirms the stepwise changing specification of ζ_S and ζ_N, Eq. (14), as reasonable approximations. The results also show that $\zeta_N = \eta^{1/2} \sim \mathrm{Ri}^{1/2}$ for $\mathrm{Ri} < 0.25$, a result found earlier by Derbyshire and Hunt (1993).

However, as for ζ_S, we find the LES results to be closer to those for salt than those for air, in spite of its subgrid-scale Prandtl number of unity. This indicates that other reasons affect the ratio of energies η. As has been discussed by Stillinger et al. (1983), Mason and Derbyshire (1990), and Yoon and Warhaft (1990), a larger fraction of vortical motions relative to wavy motions increases η. Hence, one possible reason for large values of η in the LES may be that the simulated flow contains relatively little wavy motions compared to vortical motions.

4. Discussion

a. Turbulent diffusivities

For given vertical velocity variance and mean gradients, Eq. (19) may be used to estimate the vertical diffusivities, $K_m = c_S \mathrm{Pr}_t w'^2/S$ and $K_h = c_N w'^2/N$. Alternatively, for given dissipation rate, Eqs. (9) and (10) predict $K_m = c_m \epsilon/S^2$ and $K_h = c_h \epsilon/N^2$. The equivalence of these relations was not noted before. From these equations and Table 3, we see that the coefficients are strong functions of Ri.

Hunt et al. (1985) postulated that c_N is a constant, but their measurements indicate large scatter (see Fig. 9). In fact, the present model appears to interpolate the data at least as well as a constant value of c_N. Later, Derbyshire and Hunt (1993) deduced $c_N = (0.6 \pm 0.15)\,\mathrm{Ri}^{1/2}$ for $0 < \mathrm{Ri} \leq 0.15$, and $c_N \cong 0.23 \pm 0.02$ for $\mathrm{Ri} > 0.15$. For small Richardson numbers we find the same trend, but smaller values of c_N for $\mathrm{Ri} > 0.2$.

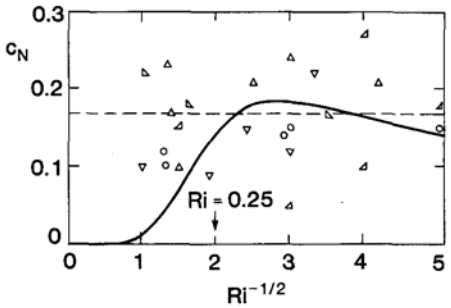

FIG. 9. Thermal diffusivity parameter $c_N = K_h N/w'^2$ versus $S/N = \mathrm{Ri}^{-1/2}$. Data of Hunt et al. (1985) in the atmospheric boundary layer. The arrow marks $\mathrm{Ri} = 0.25$. The full curve corresponds to Eq. (20) for air.

Equation (9), $K_m = c_m \epsilon/S^2$, was derived by Gregg (1987) for stationary turbulence with $G = 1$. He discusses the difficulties in applying this "dissipation method" for cases with fluctuating shear. Several previous authors assumed that the mixing efficiency $c_h = \text{const} \cong \mathrm{Ri}_f(1 - \mathrm{Ri}_f)^{-1}$ to determine the vertical diffusivity of scalar components from $K_h = c_h \epsilon/N^2$. For example, Lilly et al. (1974) assume $\mathrm{Ri}_f = 1/4$ so that $c_h = 1/3$. Osborn (1980) proposes $c_h \cong 0.2$. Weinstock (1992) revised some previous estimates and deduced that c_h is a function of the Froude and Reynolds numbers and typically about 0.17. Itsweire et al. (1993) find that $c_h = 0.16$ gives a reasonable approximation to results obtained near $\mathrm{Ri} = \mathrm{Ri}_s$ from DNS of homogeneous stratified shear turbulence at rather moderate Reynolds numbers. On the other hand, Holloway (1988) argued that previous theories give a considerable uncertainty in c_h. Equation (10) shows that c_h is not a constant. It would be constant only if $\mathrm{Ri}_f G$ is independent of Ri, but this product increases with Ri at small values of Ri, where $\mathrm{Ri}_f \cong \mathrm{Ri}/\mathrm{Pr}_{t0}$, and decreases at large values of Ri, where $G(\mathrm{Ri})$ gets very small. The

TABLE 3. Mixing coefficients $c_S = K_h S/w'^2$, $c_N = K_h N/w'^2$, $c_h = K_h N^2/\epsilon$, and $c_m = K_m S^2/\epsilon$, according to Eqs. (9), (10), and (20), for air and saltwater.

	Air				Saltwater			
Ri	c_S	c_N	c_h	c_m	c_S	c_N	c_h	c_m
0	0.75	0	0	1.47	1.20	0	0	1.80
0.1	0.58	0.18	0.12	1.22	0.87	0.27	0.18	1.47
0.2	0.38	0.17	0.15	0.94	0.48	0.21	0.20	1.04
0.3	0.23	0.13	0.14	0.69	0.25	0.14	0.16	0.69
0.4	0.14	0.09	0.11	0.50	0.13	0.08	0.11	0.46
0.5	0.09	0.06	0.09	0.36	0.07	0.05	0.08	0.31

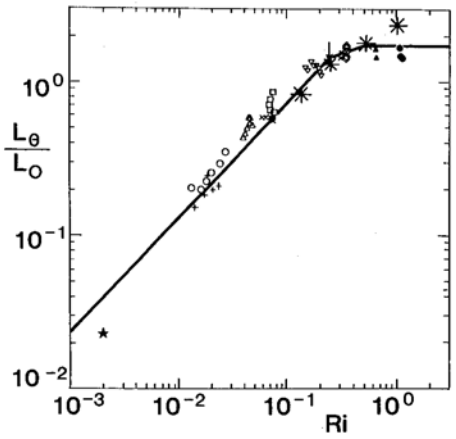

FIG. 10. Ratio of the Ellison length scale $L_\theta = \theta'/s$ to the Ozmidov length scale $L_O = \epsilon^{1/2}N^{-3/2}$ versus Ri, in logarithmic scales. Data as given by Rohr et al. (1988). The curve is the consequence of the present theory. Large stars indicate the LES results. The arrow marks Ri = 0.25.

variation is, however, not large within the range $0.1 < \mathrm{Ri} < 0.5$ (see Table 3) where the present model confirms previous findings with $c_h \cong 0.14 \pm 0.06$ for this range, both in air and saltwater.

An alternative estimate uses $K_h = c_p\epsilon_p/N^2$, which can be deduced similarly to Eq. (19) from the budget of potential energy (Osborn and Cox 1972; Gregg 1987), with $c_p \cong 1$. It is justified also by the analysis of Pearson et al. (1983), who show that the vertical diffusivity is limited by small-scale mixing of the scalar once the dispersion has extended over w'/N. Itsweire et al. (1993) find empirically that the DNS data (within ±50%) are consistent with this estimate for $c_p = 1$.

b. Relations to other mixing parameters

Our model also allows to identify several intrinsic relationships in between various mixing parameters. For example, we may determine the ratio between mixing lengths defined by

$$K_m = l_m w', \quad K_h = l_h w', \quad \epsilon = \frac{w'^3}{l_\epsilon}. \tag{33}$$

From the given relationships, we obtain

$$\frac{l_h}{l_m} = \frac{1}{\mathrm{Pr}_t}, \quad \frac{l_h}{l_\epsilon} = c_S A_S = \frac{GA_S^2}{\mathrm{Pr}_t - \mathrm{Ri}G}. \tag{34}$$

Evaluation of these functions for increasing Ri shows that the mixing length l_h for heat becomes smaller than l_m, and much smaller than the dissipation scale l_ϵ. Brost and Wyngaard (1978) assumed that the dissipation scale is limited by $l_b = w'/N$. This "buoyancy length scale" measures the vertical scale of motions that are possible under stratification for given vertical motion energy. We find, however, that the dissipation scale is not limited by the buoyancy scale, at least not for $\mathrm{Ri} < 1$, where A_S = const and

$$\frac{l_\epsilon}{l_b} = \frac{\mathrm{Ri}^{1/2}}{A_S}. \tag{35}$$

The same conclusions were obtained by Schumann (1991) from realizability conditions and numerical simulation results and by Canuto and Minotti (1993) using a spectral theory for energy transfer.

Moreover, the model predicts the ratio of Ellison scale $L_\theta \equiv \theta'/s$ to the Ozmidov scale $L_O \equiv (\epsilon/N^3)^{1/2}$ to depend only on Ri and the parameters ζ_S and A_S: $L_\theta/L_O = \zeta_S A_S^{-1/2}\,\mathrm{Ri}^{3/4}$ for $\mathrm{Ri} \leqslant 0.25$. Recently, Weinstock (1992) deduced a similar function, including the impact of limited Reynolds numbers. The linear dependence of this scale ratio on $\mathrm{Ri}^{3/4}$ is strongly supported by the data of Rohr et al. (1988) (see Fig. 10). It also agrees with DNS results of Itsweire et al. (1993). For $\mathrm{Ri} > 0.25$, our model gives $L_\theta/L_O = \zeta_N A_S^{-1/2}\,\mathrm{Ri}^{1/4}$. This is not in disagreement with the data for $\mathrm{Ri} < 0.5$. However, for even larger values of Ri, buoyancy will limit vertical motions and cause the effective length scale to be smaller than w'/S. Hence, the simple dependence of ϵ on shear alone loses validity. If $\epsilon = A_N w'^2 N$ for $\mathrm{Ri} > 0.5$, as supported by Gregg and Sanford (1988) and Tjernström (1993), with $A_N = A_S\sqrt{2}$, then one finds that $L_\theta/L_O = \zeta_N A_N^{-1/2}$ becomes independent of Ri, a result as indicated in Fig. 10. The LES results fall within the range of the measured data.

The energetics of mixing in stratified flows was also discussed by Ivey and Imberger (1991). In their theory, shear plays a secondary role compared to buoyancy forces, so that $\mathrm{Ri}_f = B/P$ becomes ill defined. Therefore, they express vertical mixing in the form of a "generalized flux Richardson number," which reads as $B(B + \epsilon)^{-1}$ in the notation of this paper. They predict a dependence of this ratio on a turbulent Froude number $\mathrm{Fr}_T = q/NL_\theta$. Using the ratio $w'^2/q^2 = 0.22$, as supported by the data of M. Tjernström (1993, personal communication), and roughly justified by Fig. 7, one can compute this Froude number from $\mathrm{Fr}_T = q/\zeta_N w'$. Both ζ_N and $B(B + \epsilon)^{-1} = \mathrm{Ri}_f GB$ can be evaluated from the present model for various values of Ri, between about 0 and 1, and plotted versus each other as in Fig. 11. The figure contains data from stratified flows, including cases without shear. The generalized flux Richardson number is maximum near $\mathrm{Fr}_T \cong 1$. For smaller Froude numbers, turbulence collapses and mixing gets very small. At larger Froude numbers, the importance of buoyancy damping decreases slowly. We find that our model equations interpolate the given data as well as the interpolation of Ivey and Imberger (1991). This provides an independent support for the present model and suggests applicability for quite a large range of stability conditions.

c. Further consequences of the dissipation model

Several authors have discussed the possibility of a constant shear number Sw'^2/ϵ. Tavoularis and Karnik

(1989) assume that this shear number is constant in neutral shear flows, while Holt et al. (1992) allow the shear number to vary. A constant shear number together with steady α_{uw} implies an exponential growth of kinetic energy, and this is clearly exhibited by Fig. 2a of Tavoularis and Karnik (1989) for Ri = 0. The present model relies on Eq. (13) with A_S = const. Hence, the assumption of a constant shear number of about 2.0 to 2.1 is supported as far as the observations agree with the model's results.

Tjernström (1993) tests a parameterization $\epsilon = q^2/\tau$ with $\tau N\sqrt{2} \cong 11$ (see Fig. 12). His measurements for ϵ, N, and q^2 can also be compared with $\epsilon = A_S w'^2 S$, for Ri < 1, and $\epsilon = A_N w'^2 N$, for Ri ≥ 1, when $w'^2/q^2 = 0.22$. This gives $\tau N\sqrt{2} = 12.86\ \mathrm{Ri}^{1/2}$, for Ri < 1, and a constant value for this parameter at stronger stratification. The data support these relations to a remarkable degree. A slightly smaller limit (Ri in between 0.5 and 0.8) between the two regimes would give even better agreement. (In Fig. 10 the limit was taken as 0.5.) The LES results fall slightly above the full curve in Fig. 12, but within the upper range of the measured data.

d. *On the turbulent Prandtl number in neutral shear flows*

Since the model depends heavily on the value $\mathrm{Pr}_t(0) = \mathrm{Pr}_{t0}$, it is appropriate to discuss various experimental and theoretical findings on this value. For saltwater, we have only the result $\mathrm{Pr}_{t0} = 0.63$ as measured by Rohr et al. (1988). Tavoularis and Corrsin (1981) find Pr_{t0} in between 1 and 1.2 from their measurements in a wind tunnel for homogeneous turbulence. Most atmospheric measurements, as discussed in Yamada (1975), Wittich and Roth (1984), Gossard and Frisch (1987), Kim and Mahrt (1992), and Tjernström (1993), show that Pr_{t0} varies in between 0.8 and 1.2. It is interesting to note, however, that Townsend (1976, section 8.9) shows that $\mathrm{Pr}_{t0} = 0.4$ in an initially isotropic turbulence field suddenly exposed to uniform shear and uniform temperature gradient and that this value increases and reaches a value of about 0.71 after a shear time St = 5 according to the rapid distortion theory. In the inertial subrange, for small departure from local isotropy, the measured values of the Kolmogorov coefficient Ko = 1.6 and the Batchelor coefficient Ba = 1.3 imply a turbulent Prandtl number of $\mathrm{Pr}_{t0} = \mathrm{Ba}(2\ \mathrm{Ko})^{-1} \cong 0.42$ (Schmidt and Schumann 1989), which is interestingly close to the isotropic limit given by Townsend (1976). Mason and Thomson (1992) show that the inertial range estimate of the turbulent Prandtl number increases to about 0.7 if one accounts for the stochastic backscatter of turbulent energy and scalar variance. Yakhot and Orszag (1986) determine $\mathrm{Pr}_{t0} = 0.72$ from the renormalization group theory, which is close to the result of Townsend for large strain. On the other hand, for anisotropic boundary layer flows with vorticity oriented in the mean flow direction, the velocity and scalar fields satisfy the same differential equations, implying $\mathrm{Pr}_t = 1$ for such flows (Liu 1992). Hence, we have to expect variations for Pr_{t0} in between 0.7 and 1.0.

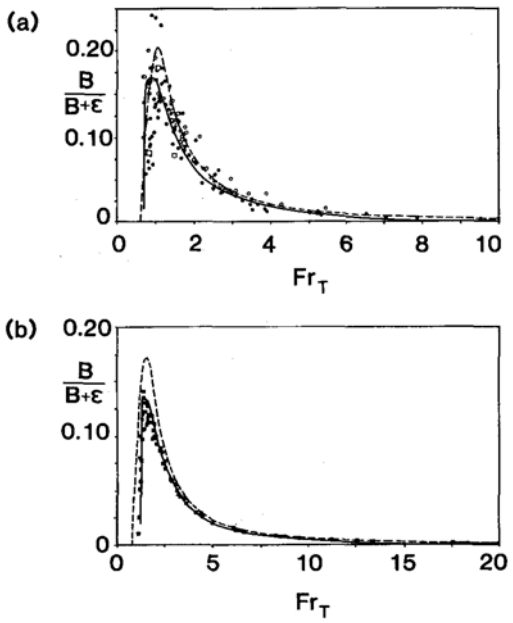

FIG. 11. Ratio of vertical buoyancy flux relative to dissipation rate $B(B + \epsilon)^{-1}$ versus the turbulent Froude number $\mathrm{Fr}_T = q\theta'/N^3 = q/w'\zeta_N$. Data as compiled by Ivey and Imberger (1991) from stably stratified flows (partly without shear). (a) For thermal diffusion (Prandtl number Pr ≈ 7) and salt diffusion (Schmidt number Sc ≈ 500) in water. (b) For thermally stratified turbulence in air (Pr ≅ 0.7). The dashed curves are from Ivey and Imberger (1991); the full curves depict the results of the present model.

From Eq. (18) we see that the correlation coefficient $\alpha_{w\theta}$ depends primarily on the product $\mathrm{Pr}_t\zeta_S$. Its values

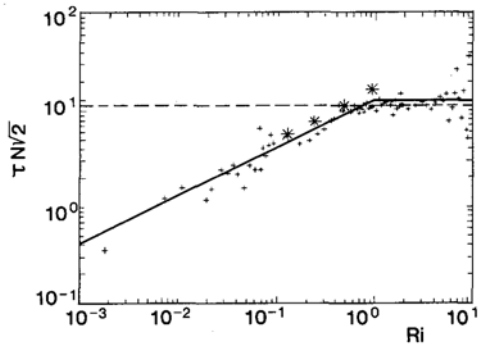

FIG. 12. The product of the timescale for dissipation $\tau = q^2/\epsilon$ and the Brunt–Väisälä frequency versus Ri. The crosses represent the measurements of Tjernström (1993), the dashed line is the model discussed by him, and the full line corresponds to the present model. Stars indicate the LES results.

1.6 in air and 2.1 in saltwater at Ri = 0 differ less than the individual factors (see Table 2) measured by Rohr (1985) and Tavoularis and Corrsin (1981). One expects that they become equal in neutral turbulent shear flows at very high Reynolds numbers.

e. *On countergradient fluxes*

The model predicts only downgradient fluxes, that is, positive terms $-\overline{uw}S$ and $-\overline{w\theta}s$. On the other hand, observations and numerical simulations have shown that countergradient transports may occur (Schumann 1987; Gerz et al. 1989; Sidi and Dalaudier 1990; Einaudi and Finnigan 1993). Formally, we obtain countergradient fluxes only if Pr_t or $G < 0$. In the absence of other sources and sinks, the kinetic and potential energy cannot decay at the same rate, since countergradient heat flux increases potential energy on the expense of kinetic energy. Such transient processes are inconsistent with the assumptions used in the present model.

Nevertheless, we have tested the model with an alternative Prandtl number function,

$$\mathrm{Pr}_t = \mathrm{Pr}_{t0}\left[\frac{\mathrm{Ri}}{\mathrm{Ri}_t - \mathrm{Ri}} + \exp\left(\frac{-\mathrm{Ri}}{\mathrm{Ri}_t - \mathrm{Ri}}\right)\right]. \quad (36)$$

This model is applicable for $\mathrm{Ri} < \mathrm{Ri}_t$, the "transition Richardson number" at the onset of countergradient heat flux. The value of Ri_t depends on the flow history and the turbulent Froude number of the flow but is often in between 0.4 and 0.8 (Komori et al. 1983; Holt et al. 1992; Kaltenbach et al. 1994). The above function describes a slowly increasing Pr_t for Ri less than about $\mathrm{Ri}_t/2$, with a strong increase above and infinite value at $\mathrm{Ri} = \mathrm{Ri}_t$. Such a dependence is well supported by the data of Rohr (1985) plotted in Fig. 3. The related flux Richardson number passes through a maximum near $0.513\,\mathrm{Ri}_t$ and becomes zero at Ri_t. We have tested the model with this function for $\mathrm{Ri}_t = 0.66$, which fits the LES result at Ri = 0.5. The results shown in Figs. 1, 2, 5, 7, 10, and 12 are independent of the Prandtl number. Only small changes occur to α_{uw}, because this depends only on the product $\mathrm{Ri}_f G$. Major changes are found for Ri > 0.25 in the trend of the heat flux correlation coefficient, which vanishes at Ri_t. As a consequence of $\mathrm{Ri}_f = 0$ at $\mathrm{Ri} = \mathrm{Ri}_t$, the model for η breaks down and predicts zero potential energy at this point. Also all the mixing coefficients c_h, c_S, and c_N become zero when the heat flux ceases. This shows that an equilibrium model, as we used in deriving η, is inconsistent with countergradient fluxes, unless there are other sources of potential energy (Schumann 1987). On the other hand, for $\mathrm{Ri} < \mathrm{Ri}_t$, the results of the present model are fairly insensitive to the precise form of the function $\mathrm{Pr}_t(\mathrm{Ri})$.

f. *Turbulence in the stable atmospheric boundary layer*

Finally, we compare the model's results with profiles of turbulence statistics measured in the stable atmospheric boundary layer. Such flows are stationary but with some finite divergence D of vertical turbulent fluxes of kinetic energy. Hence, the energy budget becomes

$$\frac{dE_k}{dt} - D = P - B - \epsilon, \quad (37)$$

with $dE_k/dt = 0$. Obviously, we can apply the given theory to this situation when we allow that $-D$ in an inhomogeneous but stationary flow takes over the role of dE_k/dt in a homogeneous but nonstationary flow case. Nieuwstadt (1984) showed that his results scale with the local Obukhov length scale Λ, and concludes that D is small compared to the other terms in the budget. He also found that the flow gets stationary for $\mathrm{Ri} \cong 0.2$, that is, at a value larger than $\mathrm{Ri}_s = 0.13$. However, Eqs. (37) and (6) give $D = (1 - G)(\epsilon + B)$. From Eq. (21) we obtain $(1 - G) = 0.19$ for Ri = 0.2. Certainly, a budget contribution of 19% by divergent upward flux of kinetic energy from the surface into the stable layer cannot be ruled out based on Nieuwstadt's measurements.

The present model does not predict the Richardson number as a function of altitude. Hence, for comparison, we apply the relationship

$$\mathrm{Ri} = \left(0.74 + 4.7\,\frac{z}{\Lambda}\right)\frac{z}{\Lambda}\left(1 + 4.7\,\frac{z}{\Lambda}\right)^{-2} \quad (38)$$

to determine $\mathrm{Ri}(z/\Lambda)$ for given altitude z relative to the Obukhov length scale Λ. This function was deduced from measurements by Caughey et al. (1979), and it also fits the measurements of Nieuwstadt (1984) (see Fig. 13a). For given $\mathrm{Ri}(z/\Lambda)$, one can compute the correlation coefficients for momentum and heat flux from Eqs. (17) and (18) and plot the results in the same format as Nieuwstadt presented his experimental data and those of Caughey et al. (1979) (see Figs. 13b,c). Obviously, the present model gives a good approximation to the measured data for the whole range of altitudes, $0 < z/\Lambda < 4$. In Fig. 13b, the new interpolation shows an increase of $1/\alpha_{uw}$ at small altitudes z/Λ, which seems to be supported even better by the data than the constant value that resulted from the second-order closure (SOC) model of Brost and Wyngaard (1978) used by Nieuwstadt. If we would apply our model with $G = 1$ instead of variable $G(\mathrm{Ri})$, the curve in Fig. 13b would show the opposite trend with decrease at small z/Λ. This shows the importance of contributions from D to the budget of kinetic energy.

5. Conclusions

A simple set of model equations has been deduced to estimate turbulent mixing in sheared and stratified

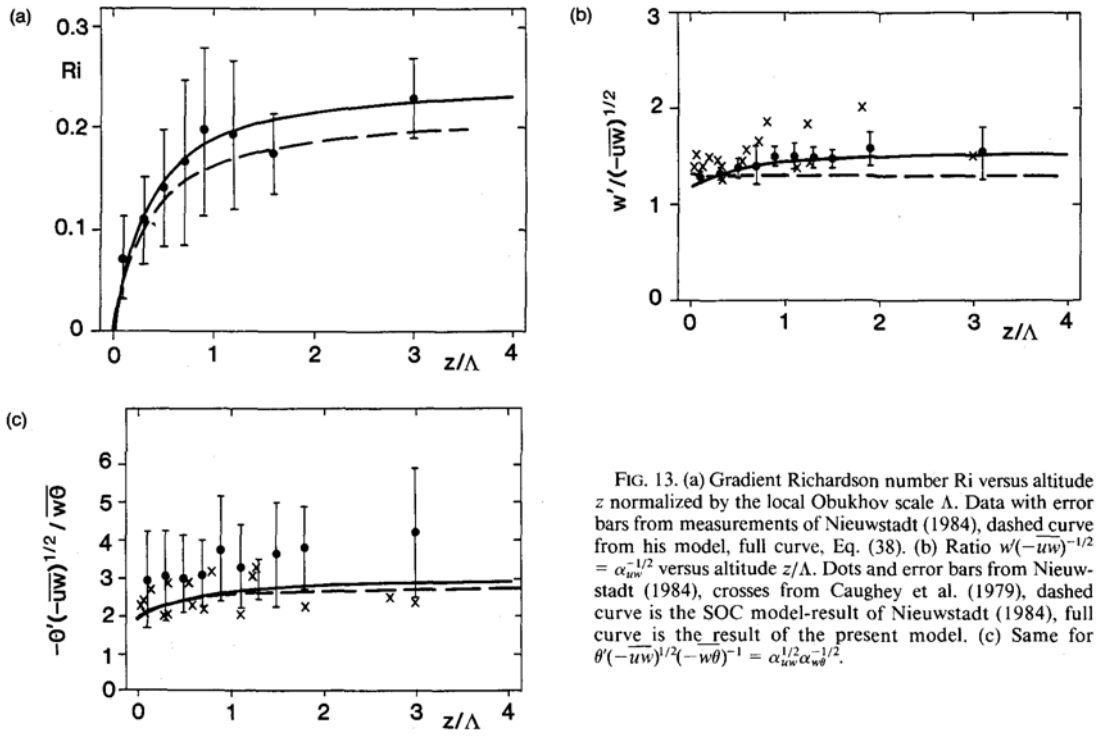

FIG. 13. (a) Gradient Richardson number Ri versus altitude z normalized by the local Obukhov scale Λ. Data with error bars from measurements of Nieuwstadt (1984), dashed curve from his model, full curve, Eq. (38). (b) Ratio $w'(-\overline{uw})^{-1/2} = \alpha_{uw}^{-1/2}$ versus altitude z/Λ. Dots and error bars from Nieuwstadt (1984), crosses from Caughey et al. (1979), dashed curve is the SOC model-result of Nieuwstadt (1984), full curve is the result of the present model. (c) Same for $\theta'(-\overline{uw})^{1/2}(-w\theta)^{-1} = \alpha_{uw}^{1/2}\alpha_{w\theta}^{-1/2}$.

flows. The relations are derived under the constraints given by the budgets of kinetic and potential energy of homogeneous turbulence. The model assumes equilibrium between potential and kinetic energy and a quasi steady state with constant decay rates and constant correlation coefficients, without countergradient fluxes. We do not expect that these conditions are satisfied always. In fact, we have shown that an equilibrium between kinetic and potential energy at high Richardson numbers, where G becomes very small, requires equal dissipation timescales for kinetic and potential energy. These timescales will not be equal in general. For closure of the model equations, we follow the suggestion of Hunt et al. (1988), relating the dissipation linearly to vertical velocity variance and shear with a coefficient A_S. A constant value of A_s is confirmed up to Ri of about 0.5–1.0. Above that limit, some data suggest that dissipation scales with w'^2N. The fluctuations of temperature of scalar concentrations vary with shear and a constant value ζ_S below Ri = 0.25, and with stratification and a constant value of ζ_N above that limit. Here, the assumption of constant ζ_S in the shear regime appears to be new. Dissipation scales with shear over a larger range of Richardson numbers than temperature fluctuations. Obviously, the large-scale buoyant scalar fluctuations experience stratification effects earlier than the smaller dissipating motions. Finally, we assume that the growth rate G decays about exponentially with Ri, and the turbulent Prandtl number Pr_t increases slowly from Pr_{t0} in between 0.7 and 1.0. For large Richardson numbers, in equilibrium conditions, $\mathrm{Pr}_t \to 4$ Ri is reasonable. Certainly, the list of assumptions is long and the model concept, therefore, does not cover all situations in real turbulent flows that are often inhomogeneous, intermittent, and strongly affected by gravity waves. However, the general agreement between the model and the observations shows that these assumptions are suitable at least for those cases for which the data were obtained.

The gap of data for homogeneous stratified shear flows in air is bridged by results from LES. The LES is used to fit Ri_s. For this purpose, we rely only on the numerical results for $\mathrm{Ri} < 0.25$, which are less sensitive to the subgrid-scale model and the numerical details than the results for larger values of Ri. The suitability of the LES results is supported by the agreement with measurements in the stable atmospheric boundary layer.

As to be expected, the model coefficients are different in stratified flows for saltwater and air because of different molecular mixing properties. However, the variations for neutral flows indicate that the database may still not represent very high Reynolds number flows. Also, some of the variations at large Richardson numbers will result from changes in the flow structures, such as wavy and vortical motion components, which cannot be predicted with the simple model.

The model estimates vertical momentum and heat fluxes by turbulence for Richardson numbers from 0 to about 1. Although only approximative, the estimates may be of practical relevance. However, either ϵ or w' has to be known from measurements or more complete models. The present concept is more general than previous ones, for example, by Lilly et al. (1974), Osborn (1980), and Hunt et al. (1985), which relate mixing with either ϵ or w', and N, and, hence, are restricted to cases with strong stratification. These estimates contain coefficients that depend strongly on Ri, mainly because of their dependence on G. At best, the coefficient $c_h = K_h N^2/\epsilon$ is approximately constant in the limits $0.1 < \mathrm{Ri} < 0.5$: $c_h \cong 0.14 \pm 0.06$. For the stable atmospheric boundary layer in steady state, where $\mathrm{Ri} < 0.22$, our results are similar to those of Derbyshire and Hunt (1993).

The analysis corroborates Nieuwstadt (1984), who found only small deviations from local equilibrium in the stable atmospheric boundary layer, but the vertical energy flux divergence may amount to about 0.2 of the energy sink. This added energy source causes a slight increase of the stationary Richardson number compared to that in homogeneous flows.

Several further implications have been found as consequences of the scaling with ϵ, w', S, and N, like the constancy of the shear number, the dependence of the heat flux correlation coefficient on the product $\zeta_S \mathrm{Pr}_t$, the reduction of l_h/l_ϵ with Ri, the increase of the ratio of Ellison's lengthscale to Ozmidov's length scale with Ri, the implicit dependence of $B(B+\epsilon)^{-1}$ on a turbulent Froude number, the increase of $\tau N = q^2 N/\epsilon$ with $\mathrm{Ri}^{1/2}$, and others, which were not noted before. Generally, the model supports in understanding and predicting transport and dissipation properties of stratified shear flows.

Acknowledgments. We greatly appreciate the work of Hans Kaltenbach, which made this study possible. We are grateful for comments from him and from Hiroshi Kawamura and Frans T. M. Nieuwstadt, which helped us to improve draft versions of this paper. We also received helpful comments by two anonymous reviewers and Michael Tjernström, which we used for further improving the paper. This work was partly supported by the Deutsche Forschungsgemeinschaft.

APPENDIX

Method and Parameters Used for the Large-Eddy Simulation

Except for the subgrid-scale (SGS) model, the method used is basically as described in Gerz et al. (1989) and therefore only the essential features are summarized here. The method simulates the turbulent flow in a cubic domain with side lengths L. The mean velocity $(U, 0, 0)$ and the mean temperature Θ have uniform gradients in the vertical coordinate z while being constant in the two other directions. All mean gradients stay constant in time because of zero divergence of fluxes in the homogeneous flow. The turbulent fluctuations relative to these mean values are $u_i = (u, v, w)$ for velocity and θ for temperature. These quantities satisfy periodic boundary conditions at the lateral sides of the computational domain and shear-periodic conditions (i.e., periodicity in a direction which rotates with the mean shear) at the upper and lower boundary. The SGS turbulent transport is modeled using the turbulent diffusivities

$$\nu_t = (c_{\mathrm{SGS}}\Delta)^2 (2S_{ij}S_{ji})^{1/2}, \quad \gamma_t = \frac{\nu_t}{\mathrm{Pr}_{\mathrm{SGS}}}, \quad \text{(A1)}$$

for velocity and temperature, respectively. Here, $S_{ij} = \partial u_i/\partial x_j + \partial u_j/\partial x_i$ is the resolved velocity deformation tensor, $c_{\mathrm{SGS}} = 0.17$ is the Smagorinsky coefficient, based on inertial subrange theory, and $\mathrm{Pr}_{\mathrm{SGS}} = 1$ is the turbulent Prandtl number of SGS motions. The simulations are performed with 128^3 equidistant grid points. An inertial subrange is not yet resolved with this resolution, so that the SGS model is only partly justified. More accurate simulations would require a much wider range of scales to be included in the LES, but this was not feasible on the computers available for this study.

The initial conditions are taken from a previous run for isotropic turbulence with maximum energy at a wavelength $L/9$. The initial flow field is fully turbulent with no coherent wave components. The turbulence intensity is $q = 0.0260\,SL$, and the integral lengthscale is $l = 0.0261\,L$. The temperature fluctuations are set to zero initially. Such fluctuations develop quickly due to vertical motions in the stratified fluid.

Simulations have been performed for Richardson numbers Ri = 0, 0.13, 0.25, 0.5, and 1. The results of the simulations are evaluated in terms of mean values that are averages over the computational domain and that are functions of time. Mean values and standard deviations of normalized quantities, as listed in Table 1, are obtained by averaging over the time period $8 < \mathrm{St} \leq 12$. In this time period the structure of the turbulent motions and statistics of correlation coefficients become approximately stationary.

The LES results are close to those obtained by DNS in Gerz et al. (1989) and Holt et al. (1992). Details are documented in Kaltenbach (1992) for LES results computed with 96^3 grid points. The present results for 128^3 grid points are fully described in Kaltenbach et al. (1994). By comparing the results with different spatial resolutions and with different SGS models, it has been shown that the results are insensitive to model details for $\mathrm{Ri} \leq 0.25$ (Gerz and Palma, 1994). Larger sensitivity to model details and initial conditions is found, as to be expected, for very stable flows with wavy motion components and a trend toward collapsed turbulence, but these results are not used for calibration of the model described in this paper.

REFERENCES

Brost, R. A., and J. C. Wyngaard, 1978: A model study of the stably stratified planetary boundary layer. *J. Atmos. Sci.*, **35,** 1427–1440.

Canuto, V. M., and F. Minotti, 1993: Stratified turbulence in the atmosphere and oceans: A new subgrid model. *J. Atmos. Sci.*, **50,** 1925–1935.

Caughey, S. J., J. C. Wyngaard, and J. C. Kaimal, 1979: Turbulence in evolving stable boundary layer. *J. Atmos. Sci.*, **36,** 1041–1052.

Derbyshire, S. H., and J. C. R. Hunt, 1993: Structure of turbulence in stably stratified atmospheric boundary layers: Comparison of large-eddy simulations and theoretical models. *Waves and Turbulence in Stably Stratified Flows,* S. D. Mobbs and J. C. King, Eds., Clarendon Press, 23–59.

Einaudi, F., and J. J. Finnigan, 1993: Wave-turbulence dynamics in the stably stratified boundary layer. *J. Atmos. Sci.*, **50,** 1841–1864.

Farrell, B. F., and P. J. Ioannou, 1993: Transient development of perturbations in stratified shear flow. *J. Atmos. Sci.*, **50,** 2201–2214.

Fernando, H. J. S., 1991: Turbulent mixing in stratified fluids. *Annu. Rev. Fluid Mech.*, **23,** 455–493.

Gerz, T., and U. Schumann, 1991: Direct simulation of homogeneous turbulence and gravity waves in sheared and unsheared stratified flows. *Turbulent Shear Flows 7,* F. Durst et al., Eds., Springer-Verlag, 27–45.

——, and J. M. L. M. Palma, 1994: Sheared and stably stratified homogeneous turbulence: Comparison of DNS and LES. *Proceedings First ERCOFTAC Workshop on direct and large-eddy simulation,* P. R. Voke, L. Kleises, and J. P. Chollet, Eds., Kluwer Academic Publishers, in press.

——, U. Schumann, and S. E. Elghobashi, 1989: Direct numerical simulation of stratified homogeneous turbulent shear flows. *J. Fluid Mech.*, **200,** 563–594.

Gossard, E. E., and A. S. Frisch, 1987: Relationship of the variances of temperature and velocity to atmospheric static stability—Application to radar and acoustic sounding. *J. Climate Appl. Meteor.*, **26,** 1021–1036.

Gregg, M. C., 1987: Diapycnal mixing in the thermocline: A review. *J. Geophys. Res.*, **92,** 5249–5286.

——, and T. B. Sanford, 1988: The dependence of turbulent dissipation on stratification in a diffusively stable thermocline. *J. Geophys. Res.*, **93,** 12 381–12 392.

Holloway, G., 1988: The buoyancy flux from internal gravity wave breaking. *Dyn. Atmos. Oceans,* **12,** 107–125.

Holt, S. E., J. R. Koseff, and J. H. Ferziger, 1992: A numerical study of the evolution and structure of homogeneous stably stratified sheared turbulence. *J. Fluid Mech.*, **237,** 499–539.

Hopfinger, E. J., 1987: Turbulence in stratified fluids: A review. *J. Geophys. Res.*, **92,** 5287–5303.

Hunt, J. C. R., J. C. Kaimal, and J. E. Gaynor, 1985: Some observations of turbulence structure in stable layers. *Quart. J. Roy. Meteor. Soc.*, **111,** 793–815.

——, D. D. Stretch, and R. E. Britter, 1988: Length scales in stably stratified turbulent flows and their use in turbulence models. *Stably Stratified Flows and Dense Gas Dispersion,* J. S. Puttock, Ed., Clarendon Press, 285–321.

Itsweire, E. C., J. R. Koseff, D. A. Briggs, and J. H. Ferziger, 1993: Turbulence in stratified shear flows: Implications for interpreting shear-induced mixing in the ocean. *J. Phys. Oceanogr.*, **23,** 1508–1522.

Ivey, G. N., and J. Imberger, 1991: On the nature of turbulence in a stratified fluid. Part I: The energetics of mixing. *J. Phys. Oceanogr.*, **21,** 650–658.

Kaltenbach, H.-J., 1992: Turbulente Diffusion in einer homogenen Scherströmung mit stabiler Dichteschichtung. Ph.D. dissertation, TU München, report DLR-FB 92-26 142 pp. [Available from DLR, Library, 51140 Köln, Germany.]

——, T. Gerz, and U. Schumann, 1994: Large-eddy simulation of homogeneous turbulence and diffusion in stably stratified shear flow. *J. Fluid Mech.*, in press.

Kim, J., and L. Mahrt, 1992: Simple formulation of turbulent mixing in the stable free atmosphere and nocturnal boundary layer. *Tellus,* **44A,** 381–394.

Komori, S., H. Ueda, F. Ogino, and T. Mizushina, 1983: Turbulence structure in stably stratified open-channel flow. *J. Fluid Mech.*, **130,** 13–26.

Lilly, D. K., 1967: The representation of small-scale turbulence in numerical simulation experiments. *Proceedings, IBM Sci. Comp. Symp. on Env. Sci.,* H. H. Goldstine, Ed., White Plains, NY, 195–210.

——, D. E. Waco, and S. I. Adelfang, 1974: Stratospheric mixing estimated from high-altitude turbulence measurements. *J. Appl. Meteor.*, **13,** 488–493.

Liu, J. T., 1992: Scalar transport in a longitudinal vorticity system in boundary layers. *Studies in Turbulence,* T. B. Gatski et al., Eds., Springer, 439–446.

Mason, P. J., and S. H. Derbyshire, 1990: Large-eddy simulation of the stably-stratified atmospheric boundary layer. *Bound.-Layer Meteor.*, **53,** 117–162.

——, and D. J. Thomson, 1992: Stochastic backscatter in large-eddy simulations of boundary layers. *J. Fluid Mech.*, **242,** 51–78.

Mellor, G. L., and T. Yamada, 1974: A hierarchy of turbulence closure models for planetary boundary layers. *J. Atmos. Sci.*, **31,** 1791–1806.

Miles, J. W., 1961: On the stability of heterogeneous shear flows. *J. Fluid Mech.*, **10,** 496–508.

Nieuwstadt, F. T. M., 1984: The turbulent structure of the stable, nocturnal boundary layer. *J. Atmos. Sci.*, **41,** 2202–2216.

Osborn, T. R., 1980: Estimates of the local rate of vertical diffusion from dissipation measurements. *J. Phys. Oceanogr.*, **10,** 83–89.

——, and C. S. Cox, 1972: Oceanic fine structure. *Geophys. Fluid Dyn.*, **3,** 321–345.

Pearson, H. J., J. S. Puttock, and J. C. R. Hunt, 1983: A statistical model of fluid-element motions and vertical diffusion in a homogeneous stratified turbulent flow. *J. Fluid Mech.*, **129,** 219–249.

Rohr, J. J., 1985: An experimental study of evolving turbulence in uniform mean shear flows with and without stable stratification. Ph.D. dissertation, University of San Diego, 271 pp. [Available from Department of Appl. Mech. and Engrg. Sci., Univ. of Calif., San Diego, La Jolla, CA 92093.]

——, E. C. Itsweire, K. N. Helland, and C. W. Van Atta, 1988: Growth and decay of turbulence in a stably stratified shear flow. *J. Fluid Mech.*, **195,** 77–111.

Schmidt, H., and U. Schumann, 1989: Coherent structure of the convective boundary layer derived from large-eddy simulations. *J. Fluid Mech.*, **200,** 511–562.

Schumann, U., 1987: The countergradient heat flux in stratified turbulent flows. *Nucl. Engrg. Des.*, **100,** 255–262.

——, 1991: Subgrid length-scales for large-eddy simulation of stratified turbulence. *Theor. Comput. Fluid Dynamics,* **2,** 279–290.

——, 1994: Correlations in homogeneous stratified shear turbulence. *Acta Mechanica* (Suppl.), **4,** 105–111.

Sidi, C., and F. Dalaudier, 1990: Turbulence in the stratified atmosphere: Recent theoretical developments and experimental results. *Adv. Space Res.*, **10,** 25–36.

Stillinger, D. C., K. N. Helland, and C. W. Van Atta, 1983: Experiments on the transition of homogeneous turbulence to internal waves in a stratified fluid. *J. Fluid Mech.*, **131,** 91–122.

Tavoularis, S., and S. Corrsin, 1981: Experiments in nearly homogeneous turbulent shear flow with a uniform temperature gradient. Part 1. *J. Fluid Mech.*, **104,** 311–347.

——, and ——, 1985: Effects of shear on the turbulent diffusivity tensor. *Int. J. Heat Mass Transfer,* **28,** 256–276.

——, and U. Karnik, 1989: Further experiments on the evolution

of turbulent stresses and scales in uniformly sheared turbulence. *J. Fluid Mech.*, **204,** 457–478.

Tjernström, M., 1993: Turbulence length scales in stably stratified free shear flow analyzed from slant aircraft profiles. *J. Appl. Meteor.*, **32,** 948–963.

Townsend, A. A., 1976: *The Structure of Turbulent Shear Flow.* 2d. ed., Cambridge University Press, 429 pp.

Tritton, D. J., 1977: *Physical Fluid Dynamics.* Van Nostrand Reinhold, 287–288.

Weinstock, J., 1992: Vertical diffusivity and overturning length in stably stratified turbulence. *J. Geophys. Res.*, **97,** 12 653–12 658.

Wittich, K.-P., and R. Roth, 1984: A case study of nocturnal wind and temperature profiles over the inhomogeneous terrain of northern Germany with some considerations of turbulent fluxes. *Bound.-Layer Meteor.*, **28,** 169–186.

Woods, J. D., 1969: On Richardson's number as a criterion for laminar–turbulent–laminar transition in the ocean and atmosphere. *Radio Sci.*, **4,** 1289–1298.

Yakhot, V., and S. A. Orszag, 1986: Renormalization group analysis of turbulence. I. Basic theory. *J. Sci. Comput.*, **1,** 3–51.

Yamada, T., 1975: The critical Richardson number and the ratio of the eddy transport coefficients obtained from a turbulent closure model. *J. Atmos. Sci.*, **32,** 926–933.

Yoon, K., and Z. Warhaft, 1990: The evolution of grid-generated turbulence under conditions of stable thermal stratification. *J. Fluid Mech.*, **215,** 601–638.